"Pile Foundation Analysis and Design

by H.G. Poulos
E.H. Davis

John Wiley and Sons. (1980)

7

ULTIMATE LATERAL RESISTANCE OF PILES

7.1 INTRODUCTION

Piles are frequently subjected to lateral forces and moments: for example, in quay and harbor structures, where horizontal forces are caused by the impact of ships during berthing and wave action; in offshore structures subjected to wind and wave action; in pile-supported earth-retaining structures; in lock structures; in transmission-tower foundations, where high wind forces may act; and in structures constructed in earthquake areas such as Japan or the West Coast of the United States, where some building codes specify that piles supporting such structures should have the ability to resist a lateral force of 10% of the applied axial load. In the design of such pile foundations, two criteria must be satisfied: first, an adequate factor of safety against ultimate failure; and second, an acceptable deflection at working loads. As in other fields of soil mechanics, these two criteria are generally treated separately, and the design is arranged to provide the required safety margins independently.

In this chapter, methods of estimating the ultimate lateral resistance of single piles and pile groups are described. In many practical cases, the design of piles for lateral loading will be dependent on satisfying a limiting lateral-deflection requirement that may result in the specificiation of allowable lateral loads much less than the ultimate lateral capacity of the piles. For such cases, the estimation of lateral deflections caused by lateral loads is discussed in Chapter 8, while the general problem of a pile or pile-group subjected to both axial and lateral loading is considered in Chapter 9. Consideration in the present chapter will be confined to situations where the lateral deflection is not an important consideration. It must, however, be emphasized that in many cases, the ultimate load will be reached at very large deflections, especially in the case of relatively flexible piles. For such cases, it may be desirable to carry out a complete elastoplastic analysis, as outlined in Section 8.3. However, for relatively rigid piles, the method described herein will generally be applicable. The chapter concludes with a brief consideration of the effects of piles on slope stability, and of methods of increasing lateral load capacity.

7.2 SINGLE PILES

In this section, methods of estimating the ultimate lateral resistance of relatively-slender vertical floating piles having negligible base resistance are considered first, and a number

(cf. Socketed piles)

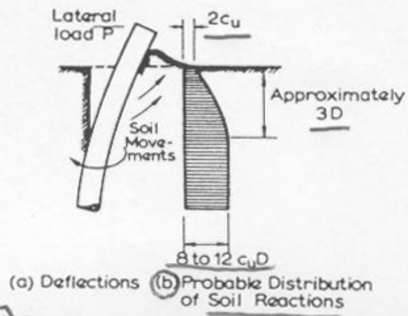

FIGURE 7.4 Distribution of lateral resistance.

c_a/c = 1 and c_a/c = 0 and, to sufficient accuracy, the solution for any intermediate value of c_a/c can be obtained by linear interpolation. The curves in Fig. 7.5 have been obtained by plasticity theory using limit analysis. (The upper bound obtained in this analysis generally only exceeded the lower bound by 10 to 15% and the curves are for the average of the two bounds). The analysis assumed the pile section to be a rhomb and may be slightly conservative for other convex shapes of the same aspect ratio. Elsewhere in this chapter the lateral resistance at depth in purely cohesive soil is usually taken as 9c, whatever the shape of the pile and value of c_a/c, see for example Brom's approach to ultimate pile capacity detailed in 7.2.2.1 below. Fig. 7.5 confirms the reasonableness of this simple assumption.

For the more general case of a $c - \phi$ soil, an alternative derivation of the ultimate lateral soil resistance, based essentially on earth-pressure theory, has been given by Brinch Hansen (1961), who also considers the variation of resistance with depth along the pile. The ultimate resistance at any depth, z, below the surface is expressed as

$$p_u = qK_q + cK_c \tag{7.8}$$

where

q = vertical overburden pressure
c = cohesion
K_c, K_q = factors that are a function of ϕ and z/d

K_c and K_q are plotted in Fig. 7.6 while the limiting values for the ground surface and for infinite depth are plotted in Fig. 7.7.

7.2.2 Broms's Theory

The theory developed by Broms (1964a and b) is essentially the same as that described in the preceding section, except that simplifications are made to the ultimate soil-resistance distribution along the pile and also that full consideration is given to restrained or fixed-head piles as well as

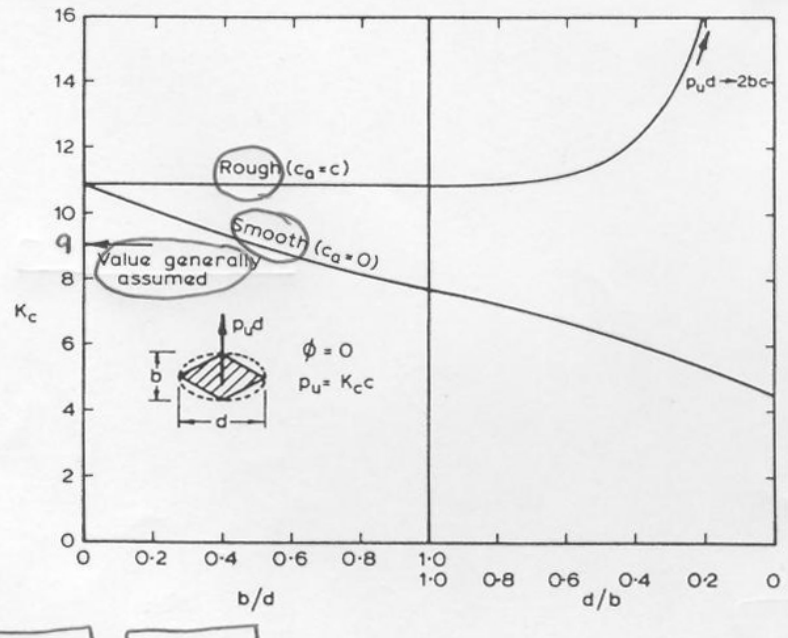

FIGURE 7.5 Effect of aspect ratio and adhesion ratio on lateral resistance for purely cohesive soil.

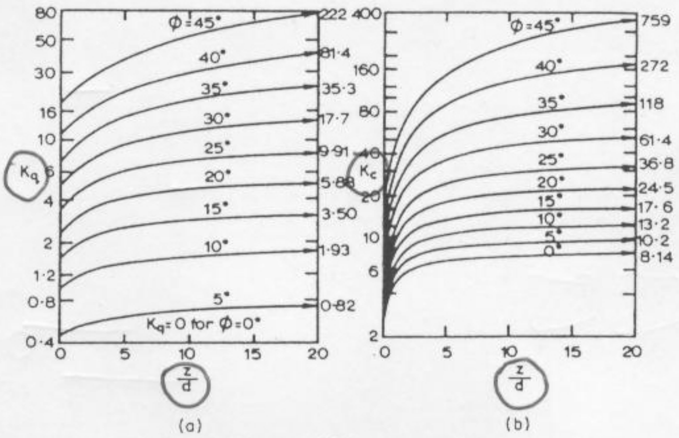

FIGURE 7.6 Lateral resistance factors K_q and K_c (Brinch Hansen, 1961).

unrestrained or free-head piles. For convenience, piles in purely cohesive soils and in purely frictional soils will be considered separately.

7.2.2.1 PILES IN COHESIVE SOILS

As discussed previously (Fig. 7.4), the ultimate soil resistance for piles in purely cohesive soils increases with depth from $2c_u$ at the surface (c_u = undrained shear-strength) to 8 to 12 c_u at a depth of about three pile-diameters ($3d$) below the surface. Broms (1964*a*) suggested a simplified distribution of soil resistance as being zero from the ground surface to a depth of $1.5d$ and a constant value of $9c_u$ below this depth. This assumes also that pile movements will be sufficient to generate this reaction in the critical zones, the location of which will depend on the failure mechanism.

dead zone

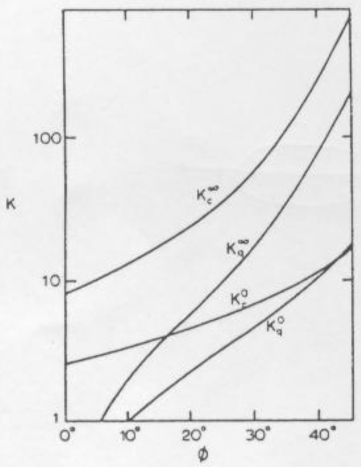

FIGURE 7.7 Lateral resistance factors at ground surface (O) and at great depth (∞) (Brinch Hansen, 1961).

Unrestrained or Free-Head Piles

Possible failure mechanisms for unrestrained piles are shown for 'short' and 'long' piles in Fig. 7.8, together with the soil-reaction distributions. 'Short' piles (termed *rigid piles* in the preceding sections) are those in which the lateral capacity is dependent wholly on the soil resistance, while 'long' piles are those whose lateral capacity is primarily dependent on the yield moment of the pile itself. In Fig. 7.8, f defines the location of the maximum moment, and since the shear there is zero,

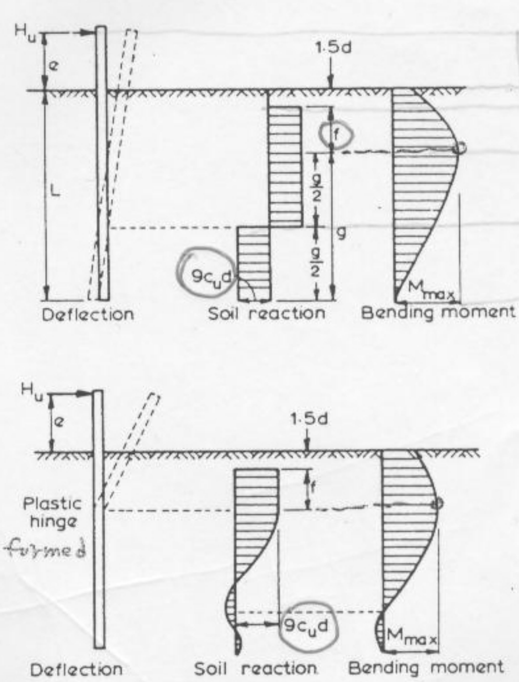

FIGURE 7.8 Failure mechanisms for piles in cohesive soil (Broms, 1964*a*).

$$f = \frac{H_u}{9c_u d} \quad \text{(7.9)}$$

H_u - ultimate horizontal load

Also, taking moments about the maximum moment location,

$$M_{\max} = H_u\,(e + 1.5d + 0.5f) \quad \text{(7.10a)}$$

also,

$$M_{\max} = 2.25dg^2c_u \quad \text{(7.10b)}$$

← short pile only

Since $L = 1.5d + f + g$, Eqs. (7.9) and (7.10) can be solved for the ultimate lateral load, H_u. The solution is plotted in Fig. 7.9a in terms of dimensionless parameters L/d and $H_u/c_u d^2$, and applies for short piles in which the yield moment $M_y > M_{\max}$, the inequality being checked by using Eqs. (7.9) and (7.10a).

For long piles, Eq. (7.10b) no longer holds, and H_u is obtained from Eqs. (7.9) and (7.10a) by setting $M_{\max}$ equal to the known value of yield moment, M_y. This solution is plotted in Fig. 7.9b in terms of dimensionless parameters $H_u/c_u d^2$ and $M_y/c_u d^3$. It should be noted that

from pile shape & material strength

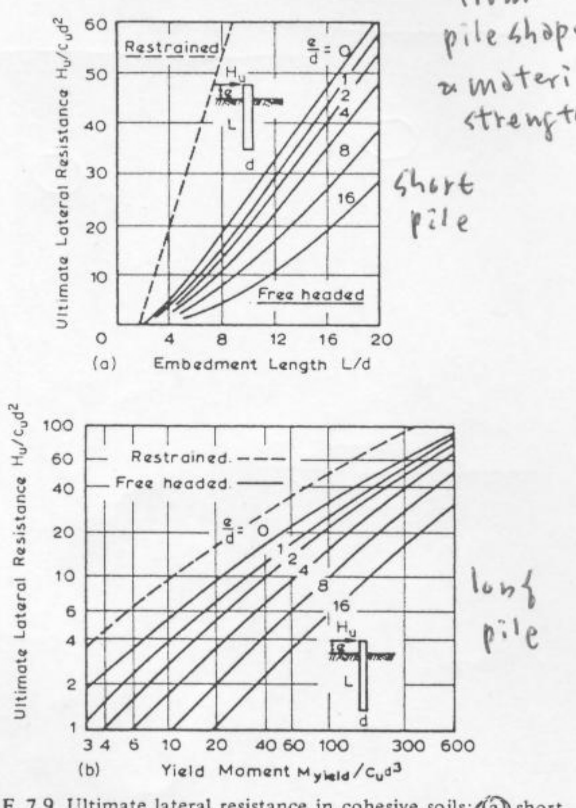

FIGURE 7.9 Ultimate lateral resistance in cohesive soils: (a) short piles; (b) lon piles (Broms, 1964a).

Broms's solution for short piles can easily be recovered from the simple statical solution for uniform soil described in Section 7.2, by using an equivalent length of pile equal to $L - 1.5d$, and an equivalent eccentricity of loading equal to $e + 1.5d$.

Restrained or Fixed-Headed Piles

Possible failure mechanisms for restrained piles are shown in Fig. 7.10, together with the assumed distributions of soil reaction and moments. The changeover points from one failure-mode to another depend again on the yield moment of the pile. It is assumed that moment-restraint equal to the

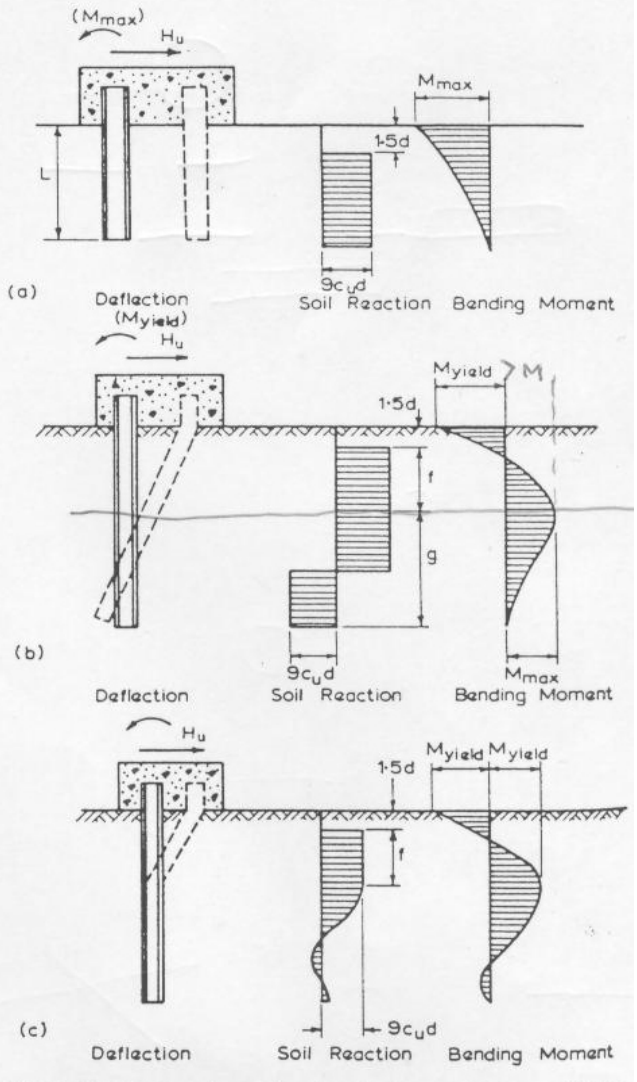

FIGURE 7.10 Restrained piles, in cohesive soil: (a) short; (b) intermediate; (c) long (after Broms, 1964a).

moment in the pile just below the cap is available*. In Fig. 7.10*a*, the following relationships hold for "short" piles:

$$H_u = 9c_u d\,(L - 1.5d) \qquad (7.11)$$

$$M_{\max} = H_u\,(0.5L + 0.75d) \qquad (7.12)$$

Solutions in dimensionless terms are shown in Fig. 7.9*a*.

For "intermediate" piles (i.e., first yield of pile occurs at the head) in Fig. 7.10*b*, Eq. (7.9) holds, and taking moments about the surface,

$$M_y = 2.25\,c_u d g^2 - 9c_u d f(1.5d + 0.5f) \qquad (7.13)$$

This equation, together with the relationship $L = 1.5d + f + g$, may be solved for H_u. It is necessary to check that the maximum positive moment, at depth $f + 1.5d$, is less than M_y; otherwise, the failure mechanism for "long" piles illustrated in Fig. 7.10*c* holds. For the latter mechanism, the following relationship applies:

$$H_u = \frac{2M_y}{(1.5d + 0.5f)} \qquad (7.14)$$

Dimensionless solutions are shown in Fig. 7.9*b*.

7.2.2.2 PILES IN COHESIONLESS SOILS

The following assumptions are made in the analysis by Broms (1964*b*):

1. The active earth-pressure acting on the back of the pile is neglected.
2. The distribution of passive pressure along the front of the pile is equal to three times the Rankine passive pressure.*
3. The shape of the pile section has no influence on the distribution of ultimate soil pressure or the ultimate lateral resistance.
4. The full lateral resistance is mobilized at the movement considered.

The simplified assumption of an ultimate soil resistance, p_u, equal to three times the Rankine passive pressure is based on limited empirical evidence from comparisons between predicted and observed ultimate loads made by Broms; these comparisons suggest that the assumed factors of 3 may in some cases be conservative, as the average ratio of predicted to measured ultimate loads is about two thirds. The distribution of soil resistance is

may be compensated by the item 4.

$$p_u = 3\sigma_v' K_p \qquad (7.15)$$

where

σ_v' = effective vertical overburden pressure
K_p = $(1 + \sin\phi')/(1 - \sin\phi')$
ϕ' = angle of internal friction (effective stress)

The analysis resulting from the assumption of the above factor of 3 is much simpler than that which would follow using Brinch Hansen's variable factor K_q (Fig. 7.6). Broms's approach is equivalent to assuming that Brinch Hansen's $K_q = 3K_p$ for all depths. From Fig. 7.7, it can be seen that for values of ϕ likely to obtain in sands, $3K_p$ lies between Brinch Hansen's surface and deep values of K_q.

Unrestrained or Free-Head Piles

Possible failure-modes, soil-resistance distributions, and bending-moment distributions for "long" and "short" piles are shown in Fig. 7.11 (for constant soil unit weight γ along the pile). As before, the pile will act as a "short" pile if the maximum moment is less than the yield moment of the section. In Fig. 7.11*a*, the rotation is assumed to be about a point close to the tip, and the high pressures acting near this point are replaced by a single concentrated force at the tip. Taking moments about the toe, *

$$H_u = \frac{0.5\,\gamma d L^3 K_p}{e + L} \qquad (7.16)$$

This relationship is plotted in Fig. 7.12*a* using the dimensionless parameters L/d and $H_u/K_p\gamma d^3$. The maximum moment occurs at a distance f below the surface, where

$$H_u = \frac{3}{2}\gamma d K_p f^2 \qquad (7.17)$$

that is,

$$f = 0.82\sqrt{\left(\frac{H_u}{dK_p\gamma}\right)}$$

The maximum moment is

$$M_{\max} = H_u\left(e + \frac{2}{3}f\right) \qquad (7.18)$$

If, after use of Eq. (7.16), the calculated value of H_u results in $M_{\max} > M_y$ ($M_{\max}$ from Eq. 7.18), then the pile

* If only limited head-restraint is available, solutions may be obtained by application of statical considerations similar to those described in this and the previous section.

* Why? D d

D >> d

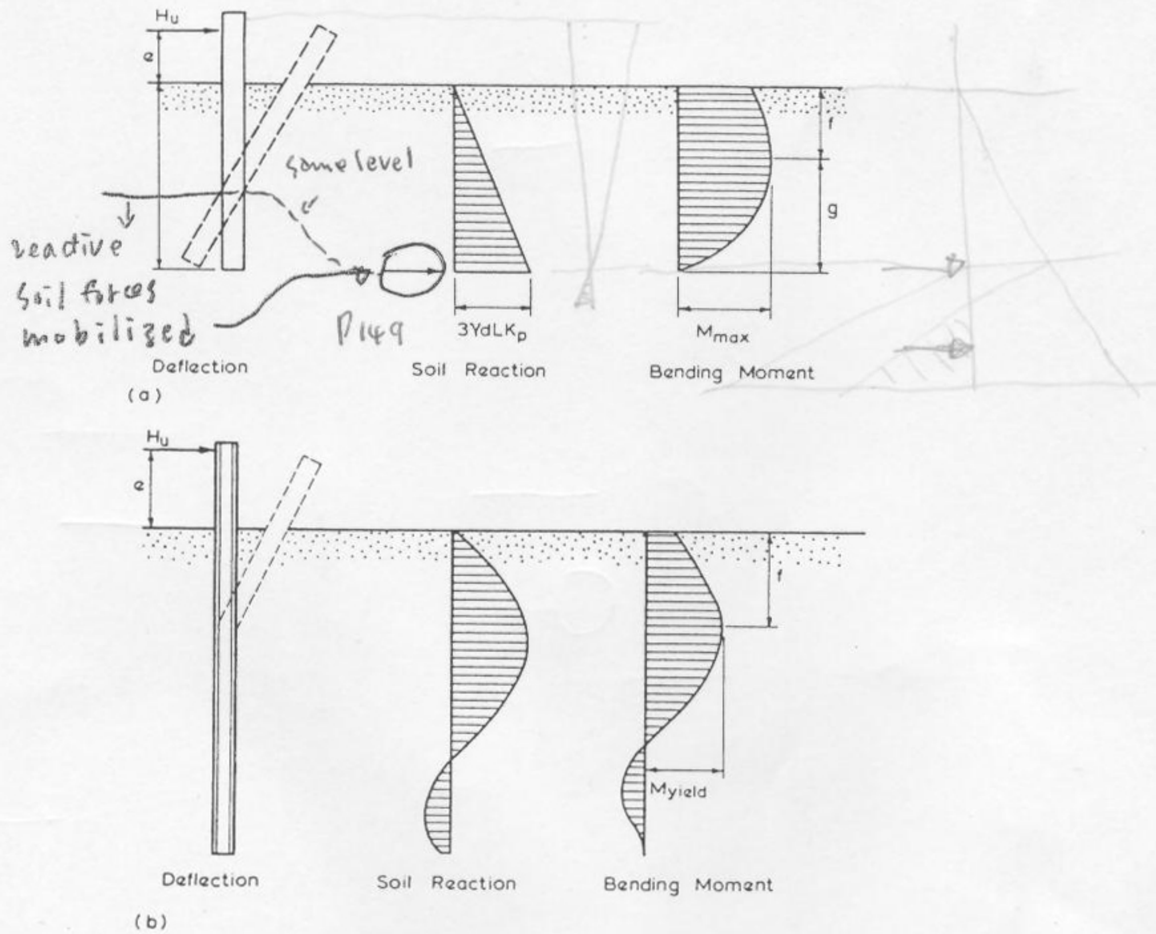

FIGURE 7.11 Free-head piles in a cohesionless soil: (a) short, (b) long (after Broms, 1964*b*).
(cf. 7.8)

will act as a "long" pile, and H_u may then be calculated from Eqs. (7.17) and (7.18), putting $M_{max} = M_y$. The solutions for H_u for "long" piles are plotted in Fig. 7.12*b*, in terms of $H_u/K_p\gamma d^3$ and $M_y/d^4\gamma K_p$.

For short piles, comparisons reveal that Broms's assumptions lead to higher values of ultimate load than the simple analysis given in Section 7.2. For example, for $L/d = 20$ and $e/L = 0$, Broms's solution gives a load 33% more than that derived from the simple statical analysis.

Restrained or Fixed-Head Piles

The assumption of an available moment-resistance at the top cap of at least M_y is again made. Possible failure modes for "short," "intermediate," and "long" piles are shown in Fig. 7.13. For a "short" pile (Fig. 7.13*a*), horizontal equilibrium gives

$$H_u = 1.5\gamma L^2 dK_p \tag{7.19}$$

This solution is plotted in dimensionless form in Fig. 7.12*a*. The maximum moment is

$$M_{max} = \frac{2}{3}H_u L \tag{7.20}$$

from soil reaction

If M_{max} exceeds M_y, then the failure mode in Fig. 7.13*b* is relevant. From Fig. 7.13*b*, for horizontal equilibrium:

$$F = \left(\frac{3}{2}\gamma dL^2 K_p\right) - H_u \tag{7.21}$$

see Fig. 13b

Taking moments about the top of the pile, and substituting for F from Eq. (7.21):

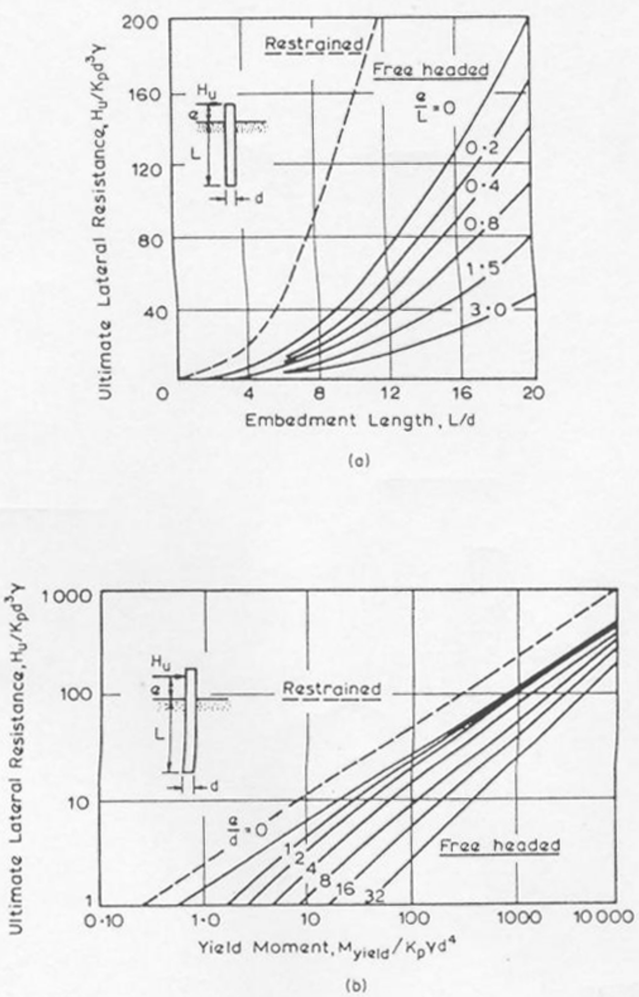

FIGURE 7.12 Ultimate lateral resistance of piles in cohesionless soils: (a) short; (b) long (after Broms, 1964*b*).

$$M_y = (0.5\gamma d\,L^3 K_p) - H_u L \qquad (7.22)$$

Hence, H_u may be obtained.
This equation only holds if the maximum moment at depth f is less than M_y, the distance f being calculated from Eq. (7.17).

For the situation shown in Fig. 7.13*c*, where the maximum moment reaches M_y at two locations, it is readily found that

$$H_u\left(e + \frac{2}{3}f\right) = 2M_y \qquad (7.23)$$

Dimensionless solutions from this equation are shown in Fig. 7.12*b*.

Comparisons have been made by Broms between maximum bending moments calculated from the above approach and values determined experimentally in a considerable number of tests reported in the literature. For cohesive soils, the ratio of calculated to observed moment ranged between 0.88 and 1.19, with an average value of 1.06. For cohesionless soils, this ratio ranged between 0.54 and 1.61, with an average value of 0.93. While good agreement was obtained, it was pointed out by Broms that the calculated maximum moment is not sensitive to small variations in the assumed soil-resistance distribution.

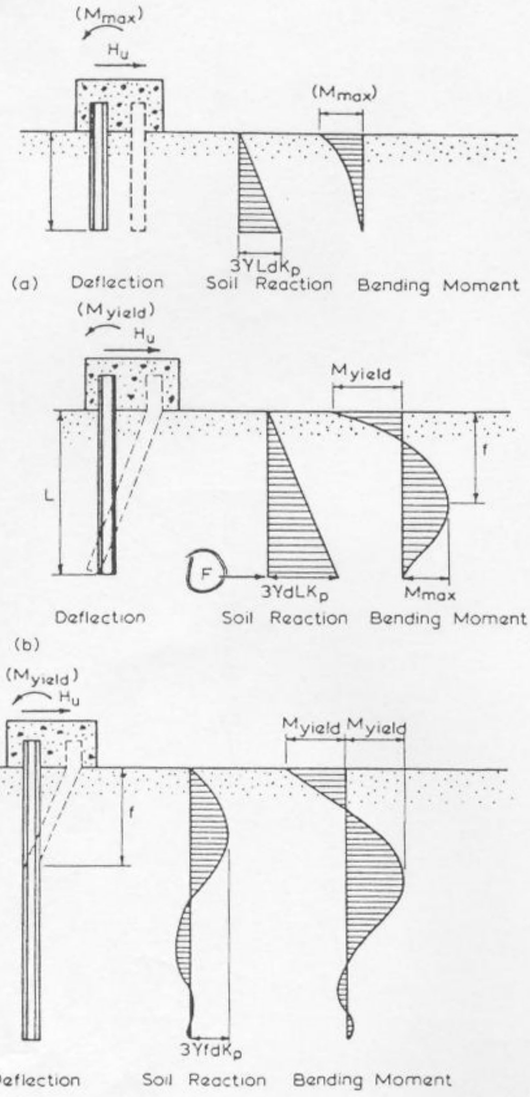

FIGURE 7.13 Restrained piles in a cohesionless soil: (a) short; (b) intermediate; (c) long.

~~7.2.3 Plane-Strain Solutions~~

Solutions for a perfectly-rigid free-head plate in a purely-cohesive weightless soil have been obtained by Davis (1961) for plane-strain conditions. If it is assumed that there can be no tension between the soil and plate and that the plate is smooth, the soil pressure will act normally over the right-hand side of a portion AB of the plate, and over the left-hand side of BC, as shown in Fig. 7.14.

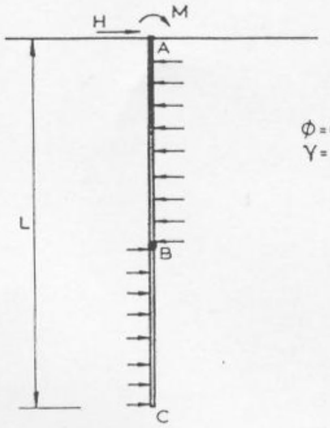

FIGURE 7.14 Plasticity analysis for laterally loaded plate.

Solutions for the failure of a strip footing near a vertical edge are then utilized. At failure, the pressure on AB is $2c$, while that on BC is given by the solution for a strip of width BC, distant AB from a vertical edge (Davis and Booker, 1973). Upper- and lower-bound solutions obtained in this way are shown in Fig. 7.15, and for practical purposes, these upper and lower bounds coincide or are only a slight distance apart. A similar approach can be employed in the case of a rough plate, by considering a rough footing under various inclinations of load (it is still assumed there is no tension between soil and plate.) A lower-bound solution for the rough-plate case is also shown in Fig. 7.15. The roughness of the plate only has an appreciable effect over a limited range of moment and load combinations. It should be emphasized that the solutions in Fig. 7.15 are for a weightless soil and will tend to be conservative for soil having appreciable weight. Also, plane-strain conditions are assumed with failure occurring in a vertical plane in contrast to failure in a horizontal plane in the analysis in Fig. 7.5. Model tests (Douglas, 1958) show satisfactory confirmation of the theory.

Comparisons between the solutions in Fig. 7.15 and those obtained from Broms's theory (Fig. 7.9) show that the ultimate lateral resistance calculated from plasticity theory is much less than that from Broms's theory—for example, for $L/d = 12$ and $e/L = 0$, the calculated ultimate loads differ by a factor of 3. This difference arises largely from the lower ultimate-soil-resistances used in the plasticity approach (a value of $2c_u$ for the portion AB and a maximum value of $5.14c_u$ for portion BC, as against Broms's value of $9c_u$), as a consequence of the assumption of plane-strain conditions.

The plasticity solutions in Fig. 7.15, while unduly conservative for normal proportions of pile, are relevant to the case of shallowly-embedded sheet piling and may be

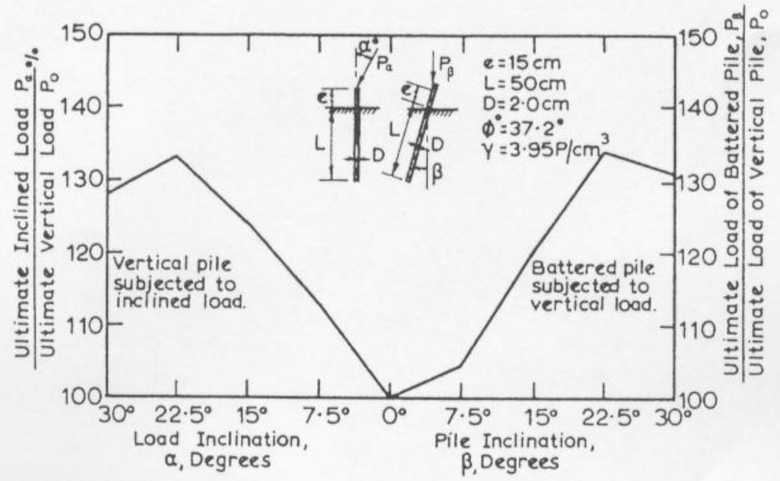

7.3 pile groups

FIGURE 7.21 Load capacity of battered piles and piles subjected to inclined load (Awad and Petrasovits, 1968).

The group capacity is the lesser of

1. n times the lateral load capacity of a single pile.
2. The lateral load capacity of an equivalent single block containing the piles in the group and the soil between them.

The first value, representing individual pile failure, can be obtained by the methods described in Section 7.2. The second value, representing block failure and occurring at relatively close spacings, can be obtained as described in Section 7.2.4 for an equivalent single pile of diameter or width equal to the breadth of the group perpendicular to the direction of loading. However, in using Broms's theory for a pile group in clay, it is clearly absurd to allow a "dead" zone of zero soil-reaction of 1.5 times the group breadth, while ignoring such a zone may be unduly optimistic. A reasonable compromise is to use a "dead" zone of the lesser of $1.5d$ (d = individual pile diameter) or $0.1L$ (L = embedded length of piles). Results of a limited series of model tests suggest that the above procedure gives a reasonable estimate of the group capacity at close spacings. It the group is relatively narrow, and loaded perpendicular to the longer direction, the ultimate lateral load for block failure may be estimated from the plasticity solutions in Fig. 7.15. For a group of fixed-head piles, with the head embedded in a massive cap, the ultimate load for block failure can be calculated as the sum of the resistance of a short restrained pile (e.g., see Fig. 7.9 and 7.12) and the shear resistance of the base. Some allowance may also be made for side shear resistance of the block.

The concept of a group efficiency for lateral loading, η_L can be employed as with group efficiency for vertical loading, where for a group of n piles,

$$\eta_L = \frac{\text{Ultimate lateral-load capacity of group}}{n \times \text{ultimate lateral load capacity of single pile}} \tag{7.35}$$

A relatively small amount of data is available for values of η_L. A series of tests on model pile groups in clay was carried out by Prakash and Saran (1967) while Oteo (1972) carried out similar tests in sand; the values of η_L derived from these test results are shown in Fig. 7.22. η_L decreases with increasing numbers of piles in a group or with decreasing spacing.

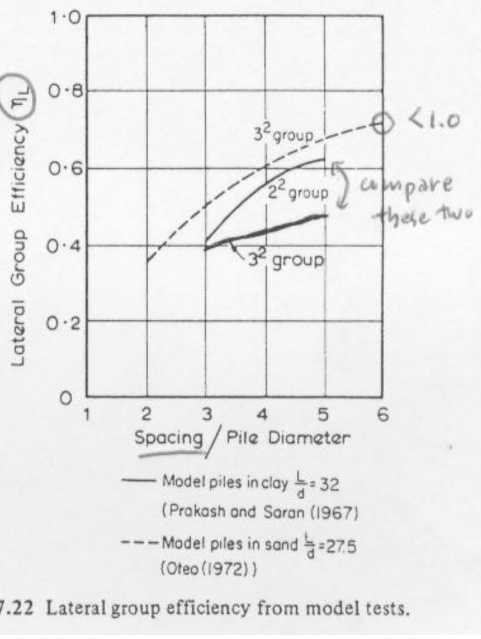

FIGURE 7.22 Lateral group efficiency from model tests.

7.11 GROUP ACTION

Piles are most often used in groups. Therefore, the value of k needs to be corrected. The following guidelines may be used.

1. If the center-to-center spacing in the direction of loading is 8 d, in which d is the diameter of the pile, and the center-to-center spacing is at least 2.5 d in the direction perpendicular to the load, there is no group action.
2. If the spacing in the direction of the load is 3 d, the effective value of k (k_{eff}) is 0.25 k. For other spacing values, a linear interpolation may be made.
3. If the load is applied in a repeated manner, the deflections increase and k_{eff} decreases. It has been observed that the deflections after 50 cycles of load application are double the deflections under the first cycle (Prakash, 1962). The soil modulus is correspondingly reduced. The deflections after 800 cycles are increased to about 2.5 to 3 times the deflections in the first cycle (Prakash and Chandrasekaran, 1970). The soil modulus is further reduced.
4. If the load is applied in an oscillatory manner, the deflections increase about seven times that under the first cycle of loading (Prakash and Sharma, 1969). The soil modulus decreases to a larger extent in this case.

If group action and oscillatory loads are considered, the soil modulus is decreased on two counts, and the final value may be less than 10 percent of k for a single pile.

These recommendations may be regarded as tentative. When more data become available, these recommendations may need to be revised.

a pile is installed in the slope, the portion of the pile (length L_1) above the assumed failure surface will be subjected to an inclined disturbing force P at some eccentricity e above this surface. Ignoring any axial resistance for simplicity, this disturbing force can be considered to be resisted by the lower portion of the pile (length L_2) below the critical failure surface. The maximum value of this resisting force, H_u, is given by the least of the following four values:

1. The ultimate lateral resistance of a "short" pile of length L_2 loaded at an eccentricity e.
2. The ultimate lateral resistance of a "long" pile loaded at an eccentricity e (this value will depend on the yield moment of the pile).
3. The ultimate load that can be developed along the upper part (length L_1) of the pile if the soil flows past the pile and the ultimate pile-soil pressure is developed along this portion of the pile.
4. The shear resistance of the pile section itself.

The values in 1, 2, and 3 may be obtained from the analysis presented in Section 7.2, once the ultimate pile-soil pressure distribution has been determined. Approximate allowance can be made for the inclination, as outlined in Section 7.2.6. The eccentricity e can, as a first approximation, be estimated by assuming full mobilization of the pile-soil pressure above the assumed failure surface.

Once the value of H_u has been thus determined, the additional resisting moment or force caused by the pile can be determined, and hence the effect on the safety factor can be evaluated (see Fig. 7.24). The procedure must be repeated for a series of trial failure surfaces to find the one with the lowest safety factor. Consideration should also be given to a surface that passes below the pile tips.

With groups of piles, adjustments can be made to the ultimate pile-soil pressures to allow for group effects, and the influence of each pile can be added up to determine the effect of the group on slope stability.

7.5 METHODS FOR INCREASING THE LATERAL RESISTANCE OF PILES

Broms (1972) has discussed some methods of increasing the lateral resistance of piles. As shown in Fig. 7.25, most of

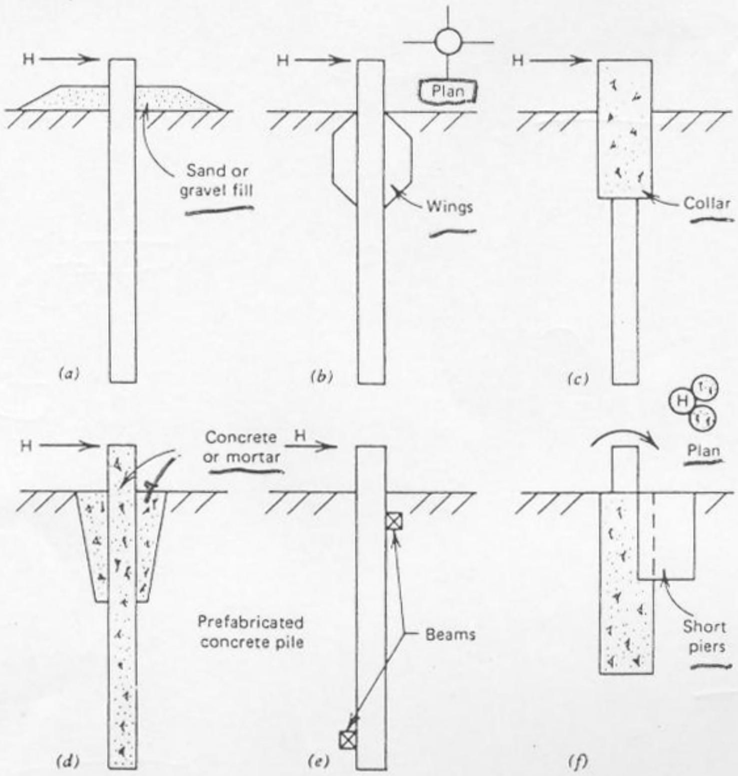

FIGURE 7.25 Methods used to increase the lateral resistance of piles.